# Second-Order Nonlinear Performance of Poly(methyl methacrylate) Films with Dispersed Donor−Acceptor Organobimetallic Compounds

**Carolina López-Garabito, Jose A. Campo, Jose V. Heras, and Mercedes Cano**

*Facultad de Químicas, Departamento Química Inorgánica, Universidad Complutense de Madrid, 28040 Madrid, Spain*

**Gema Rojo and Fernando Agulló-López***

*Facultad de Ciencias, Departamento de Física de Materiales, Universidad Autónoma de Madrid, 28049 Madrid, Spain*

*Received: June 25, 1998*

New organobimetallic Mo/Fe compounds of the type [Mo($Tp^{An}$)(NO)(Cl)(Y-$\pi$-bridge)(Fc)] {$Tp^{An}$ = hydrotris(3-*p*-methoxyphenylpyrazol-1-yl)borate; Fc = ($\eta^5$-$C_5H_4$)Fe($\eta^5$-$C_5H_5$); Y = NH (**1**), O (**5**), bridge = $C_6H_4$; Y = NH, bridge = $C_6H_3R-N{=}N-C_6H_3R'$ [R = R′ = H (**2**); R = $CH_3$, R′ = H (**3**); R = R′ = $CH_3$ (**4**); Y = NH, bridge = $C_6H_4-CH{=}CH-C_6H_4$ (**6**)} have been synthesized and characterized. The second-harmonic generation yield of corona-poled spin-coated films of poly(methyl methacrylate) containing these compounds has been investigated. The three nonzero components, $\chi^{(2)}_{31}$, $\chi^{(2)}_{15}$, and $\chi^{(2)}_{33}$, of the susceptibility tensor have been measured. $\chi^{(2)}_{31}$ is the highest component at difference with linear (one-dimensional) molecules where $\chi^{(2)}_{33} = 3\chi^{(2)}_{31}$. Moreover, Kleinman symmetry ($\chi^{(2)}_{31} = \chi^{(2)}_{15}$) is not obeyed. These results have been discussed on the basis of a low-lying charge-transfer optical transition that has a perpendicular component to the permanent dipole moment. From the measured $\chi^{(2)}$ components, the molecular hyperpolarizabilities $\beta_{33}$, $\beta_{15}$, and $\beta_{31}$ have been estimated under the assumption of thermal equilibrium under the poling field. On the other hand, the role of diverse bridging structures on the susceptibilities, including different lengths (diarylazoamide vs anilide), as well as methyl substituents and linking (C═C vs N═N) groups, has been evaluated. Moreover, the acceptor [Mo($Tp^{An}$)(NO)(Cl)(Y)] and nitro groups have been compared in compounds having the same ferrocenyl donor group and polarizable bridging system. $\chi^{(2)}_{31}$ susceptibilities are significant in most cases, and values as high as $6.6 \times 10^{-9}$ esu have been obtained for the 4-nitro-4′-ferrocenylstilbene compound.

## 1. Introduction

Presently, there is an intensive search for novel nonlinear optical (NLO) materials to design and prepare improved bulk and waveguide devices for nonlinear optical applications. Organic materials present a number of advantages over inorganic crystals because of their high and ultrafast nonlinear response and low dielectric constant, as well as the enormous design flexibility allowed by molecular engineering.[1−3] Although many organic compounds have already been investigated, some novel strategies are now being actively pursued to optimize physical and nonlinear performance. One such route is offered by the organometallic compounds[4,5] first used by Green and coworkers[6] on ferrocene derivatives. So far, relatively few second-order NLO studies have been performed on organometallic molecules, and most of them have used the Kurtz powder method.[7] Although this method is rather crude and qualitative, it has shown very promising results for some compounds. Unfortunately, it is difficult to predict and control molecular packing during crystallization, and so, the macroscopic NLO response, as measured by the Kurtz technique, is not indicative of the quadratic molecular hyperpolarizability.

Organometallic compounds have been used as acceptor or donor groups bonded by a $\pi$-conjugated electron path with the idea of increasing the hyperpolarizability $\beta$. In the last few years, complexes of the type [M($Tp^{Me2}$)(NO)(X)(Y)] (M = Mo, W; X = Cl, Br, I; Y = OR, NHR; $Tp^{Me2}$ = [HB{3,5-$(CH_3)_2$−$C_3HN_2$}$_3$]$^-$) have been shown to exhibit reversible redox behavior with a low reduction potential, which should imply efficient acceptor capabilities.[8] Therefore, compounds of the type [M($Tp^{Me2}$)(NO)(X)(Y-$\pi$-D)] (Figure 1), in which the electronically unsaturated (16e$^-$) acceptor fragments [M($Tp^{Me2}$)(NO)(X)(Y)] were bonded to a donor D group through a bridging Y-$\pi$ system, have been described, and their second-harmonic generation (SHG) response has been qualitatively evaluated with the Kurtz powder method. It is remarkable that despite the variety of compounds examined only those containing the donor ferrocenyl group exhibited significant SHG.[9−11] This fact may be explained by considering that donor and acceptor groups of similar size (e.g., both bulky) at the ends of the bridging chain contribute to a noncentrosymmetric molecular arrangement.[9] Kurtz values as high as 30, 35, 50, and 85 with respect to urea were obtained for four ferrocenyl derivatives, suggesting the ability of this type of compounds to generate high quadratic hyperpolarizabilities.[9,11]

In this work, we have focused on novel bimetallic molecules having a donor ferrocenyl (Fc) group linked through a charge-transfer (CT) axis to a 16e$^-$ acceptor Mo moiety of the type [Mo($Tp^R$)(NO)(X)(Y)]. In particular, the bulky ligand $Tp^{An}$ ([HB(3-*p*-$CH_3OC_6H_4-C_3H_2N_2)_3$]$^-$) has been used as the acceptor end instead of the previous $Tp^{Me2}$. The $Tp^{An}$ ligand is expected to maintain the favorable steric characteristics of the

10.1021/jp982764v CCC: $15.00 
Published on Web 12/04/1998

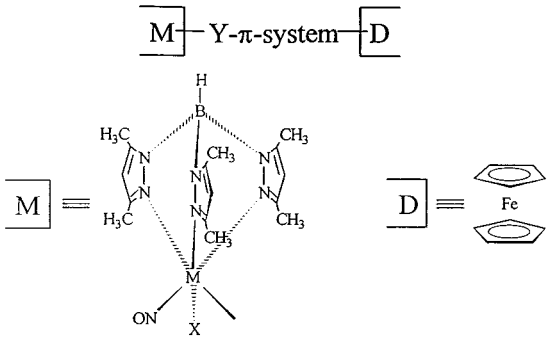


**Figure 1.** Schematic diagram for the Mo-acceptor group and bridging path to the donor.

$Tp^{Me2}$ ligand for NLO. Moreover, the additional $\pi$-conjugation at its substituents makes the investigation of its behavior worthwhile. The role of different $\pi$-bridging structures on the SHG response has been evaluated. The basic strategy was to introduce either NH or O as Y-coordinating groups, as well as bridging systems with (a) N═N or C═C groups and (b) unsubstituted or alkyl-substituted aromatic groups. A complementary objective has been to compare the acceptor strengths of the [Mo($Tp^{An}$)(NO)(Cl)(Y)] and $NO_2$ groups in complexes having the same ferrocenyl donor and bridging groups.

The chemical structures of all molecules synthesized and investigated in this work are given in Figure 2. The ground-state dipole moments measured for some of them are also included.

To assess the SHG capabilities of the new organobimetallic compounds, guest−host PMMA films have been prepared by spin-coating. The noncentrosymmetric molecular ordering has been achieved by corona poling.[12] The SHG measurements on the films have allowed for the determination of the three nonzero components, $\chi^{(2)}_{31}$, $\chi^{(2)}_{15}$, and $\chi^{(2)}_{33}$, of the second-order susceptibility tensor (considering $C_{\infty v}$ symmetry). From these data the quadratic hyperpolarizability, $\boldsymbol{\beta}$, tensor has been estimated through general statistical arguments assuming thermal equilibrium under the poling field.[13] One should remark that the experiments on ordered films do not present restrictions on $\boldsymbol{\chi}^{(2)}$ at variance with those performed on crystalline powders which are often centrosymmetric. Finally, thin films may provide suitable materials for implementation in useful waveguide and integrated optics devices.

## 2. Experimental Section

**2.1. Synthesis and Characterization.** *Materials.* The known compounds 4-ferrocenylphenol, 4-ferrocenylaniline, 4-amino-4′-ferrocenylazobenzene, 4-amino-4′-ferrocenyl-2-methylazobenzene, 4-amino-4′-ferrocenyl-2,3′-dimethylazobenzene, 4-amino-4′-ferrocenylstilbene, and 4-nitro-4′-ferrocenylstilbene were prepared using previously described procedures.[9,11,14] The starting Mo complex [Mo($Cl)_2$($Tp^{An}$)(NO)] was also obtained as reported.[15] All reaction solvents were dried and degassed according to standard methods.

Reactions were carried out under an atmosphere of dry oxygen-free dinitrogen, but the reaction products were handled in air. Silica gel 60 (70−230 mesh) was used for all chromatographic separations.

*Physical Measurements.* Elemental analyses were carried out by the Center for Elemental Microanalysis at the Complutense University in Madrid. Fast atom bombardment mass spectra were obtained on a VG AutoSpec spectrometer. Infrared spectra were recorded on a Fourier transform infrared Nicolet Magna-550 spectrophotometer with the compounds in KBr disks in the 4000−350-$cm^{-1}$ region.

$^1$H and $^{13}$C NMR spectra were performed on a Varian VXR-300 (299.88 and 75.40 MHz for $^1$H and $^{13}$C, respectively) or a Bruker AM-300 (300.13 and 75.43 MHz for $^1$H and $^{13}$C, respectively) spectrophotometers from solutions in $CDCl_3$. Chemical shifts, $\delta$, are listed in parts per million relative to tetramethylsilane; coupling constants, $J$, are in hertz. The $^1$H and $^{13}$C chemical shifts are accurate to 0.01 and 0.1 ppm, respectively; coupling constants are accurate to ±0.3 Hz for $^1$H NMR spectra. The full assignation of the proton resonances was made by proton homonuclear decoupling techniques using the latter spectrophotometer. The nomenclature of the atoms used in the assignation of the NMR signals is shown in Figure 2.

Cyclic voltammetric experiments were carried out on an Autolab apparatus equipped with a PSTA10 potentiostat. Solutions were ca. $10^{-3}$ and 0.2 mol·$dm^{-3}$ in [$NBu^n_4$][$BF_4$] as the base electrolyte. A three-electrode cell was used with a scan rate of 200 mV·$s^{-1}$. Potentials were quoted relative to a Ag/AgCl electrode as a reference, and ferrocene was used as an internal standard.

UV−vis spectra for solutions in dichloromethane were recorded with a Cary 5G spectrophotometer.

*Synthetic Methods. [Mo(Cl)($Tp^{An}$)(NO){$NHC_6H_4$-4-($\eta^5$-$C_5H_4$)-Fe($\eta^5$-$C_5H_5$)}] (**1**).* A solution of [Mo($Cl)_2$($Tp^{An}$)(NO)] (0.26 g, 0.34 mmol), 4-ferrocenylaniline (0.11 g, 0.40 mmol), and triethylamine (0.50 $cm^3$, 3.65 mmol) was stirred under reflux in toluene (50 $cm^3$) for 6 h. The solution color changed from brownish red to greenish black. Then, the reaction mixture was cooled and evaporated to dryness under reduced pressure. The resulting solid was purified by column chromatography on silica gel using 4% methanol−dichloromethane as the eluent. The major greenish black band was collected, yielding the brownish black product (0.2 g, 61%).

*[Mo(Cl)($Tp^{An}$)(NO){$NHC_6H_4$[N═$NC_6H_4$-4-($\eta^5$-$C_5H_4$)Fe($\eta^5$-$C_5H_5$)]-4}] (**2**).* A solution of [Mo($Cl)_2$($Tp^{An}$)(NO)] (0.17 g, 0.23 mmol), 4-amino-4′-ferrocenylazobenzene (0.09 g, 0.23 mmol), and triethylamine (0.23 $cm^3$, 1.67 mmol) was stirred under reflux in toluene (15 $cm^3$) for 5 h. The solution color changed from brownish red to deep purple. Then, the reaction mixture was cooled and evaporated to dryness under reduced pressure. The resulting solid was purified by column chromatography on silica gel using 1% tetrahydrofurane−dichloromethane as the eluent. The major purple band was collected, yielding the deep purple product (0.2 g, 79%).

*[Mo(Cl)($Tp^{An}$)(NO){$NHC_6H_3$(3-$CH_3$)[N═$NC_6H_4$-4-($\eta^5$-$C_5H_4$)-Fe($\eta^5$-$C_5H_5$)]-4}] (3).* The compound was prepared in a manner identical to that of **2**, using [Mo($Cl)_2$($Tp^{An}$)(NO)] (0.36 g, 0.49 mmol), 4-amino-4′-ferrocenyl-2-methylazobenzene (0.20 g, 0.50 mmol), and triethylamine (0.50 $cm^3$, 3.70 mmol). Tetrahydrofurane−dichloromethane (1.5%) was employed as the eluent, yielding a deep purple solid (0.17 g, 77%).

*[Mo(Cl)($Tp^{An}$)(NO){$NHC_6H_3$(3-$CH_3$)[N═$NC_6H_3$(3-$CH_3$)-4-($\eta^5$-$C_5H_4$)Fe($\eta^5$-$C_5H_5$)]-4}] (**4**).* The compound was prepared in a manner identical to that of **2**, using [Mo($Cl)_2$($Tp^{An}$)(NO)] (0.14 g, 0.20 mmol), 4-amino-4′-ferrocenyl-2,3′-dimethylazobenzene (0.08 g, 0.20 mmol), and triethylamine (0.19 $cm^3$, 1.42 mmol). A deep purple solid was obtained (0.16 g, 70%).

*[Mo(Cl)($Tp^{An}$)(NO){$OC_6H_4$-4-($\eta^5$-$C_5H_4$)Fe($\eta^5$-$C_5H_5$)}] (**5**).* A solution of [Mo($Cl)_2$($Tp^{An}$)(NO)] (0.51 g, 0.67 mmol), 4-ferrocenylphenol (0.23 g, 0.83 mmol), and hexamine (0.05 g, 0.36 mmol) was stirred under reflux in toluene (40 $cm^3$) for 5 h. The solution color changed from brownish red to purple. Then, the reaction mixture was cooled and evaporated to dryness under

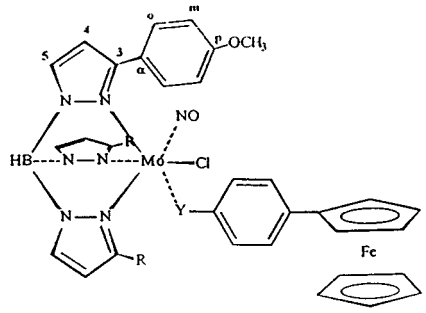

Y= NH (1)
O (5)

$\mu^{(0)} = 10.8$ Debyes

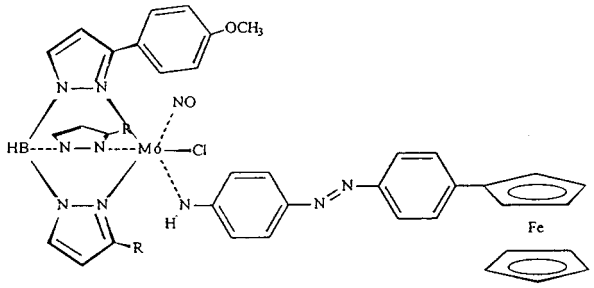

(2)

$\mu^{(0)} = 10.2$ Debyes

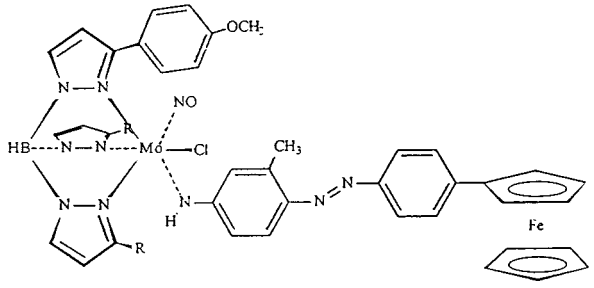

(3)

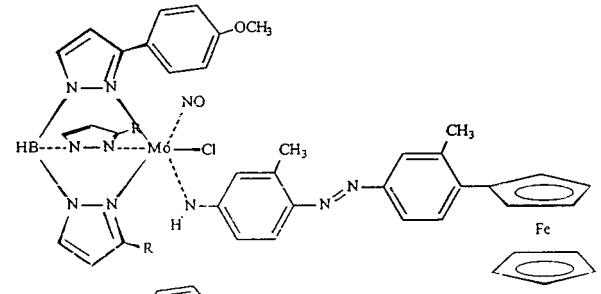

(4)

$\mu^{(0)} = 10$ Debyes

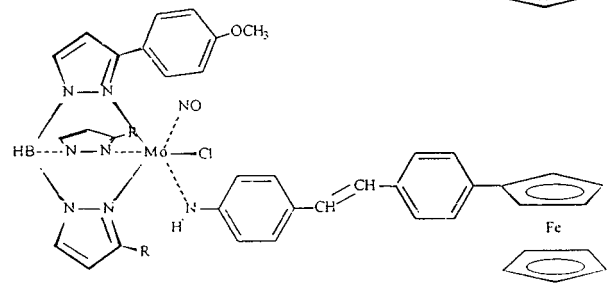

(6)

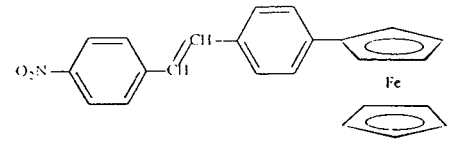

(7)

R= $CH_3OC_6H_4$

**Figure 2.** Molecular structures for compounds **1**−**7**. Ground-state dipole moments measured for some molecules are also included.

reduced pressure. The resulting solid was purified by column chromatography on silica gel using 2% methanol−dichloromethane as the eluent. The major purple band was collected, yielding the deep purple product (0.4 g, 61%).

*[Mo(Cl)(Tp$^{An}$)(NO){NHC$_6$H$_4$[CH═CHC$_6$H$_4$-4-($\eta^5$-C$_5$H$_4$)Fe($\eta^5$-C$_5$H$_5$)]-4}] (**6**).* A solution of [Mo(Cl)$_2$(Tp$^{An}$)(NO)] (0.15 g, 0.20 mmol), 4-amino-4′-ferrocenylstilbene (0.08 g, 0.21 mmol), and triethylamine (0.40 cm$^3$, 2.90 mmol) was stirred under reflux in toluene (60 cm$^3$) for 4 h. The solution color changed to purple. Then, the reaction mixture was cooled at room temperature and evaporated to dryness under reduced pressure. The resulting solid was purified by column chromatography on silica gel using 5% methanol−dichloromethane as the eluent. The major purple band was collected, yielding a deep purple solid (0.16 g, 76%)

*Characterization. Complex **1**.* Found: C, 57.58; H, 4.73; N, 10.97. Calcd for MoFeClBC$_{46}$H$_{42}$N$_8$O$_4$: C, 57.01; H, 4.34; N, 10.57. IR (cm$^{-1}$): $\nu$(NH) 3277; $\nu$(BH) 2477; $\nu$(NO) 1671. Mass spectrum (*m*/*z*, assignation): 970 [M]$^+$, 935 [M − Cl]$^+$, 656 [M − Cl − {NHC$_6$H$_4$-4-($\eta^5$-C$_5$H$_4$)Fe($\eta^5$-C$_5$H$_5$)}]$^+$, 277 [H$_2$NC$_6$H$_4$-4-($\eta^5$-C$_5$H$_4$)Fe($\eta^5$-C$_5$H$_5$)]. Cyclic voltammetry [$E_{1/2}$, V; ($\Delta E$, mV)]: −0.906 (150), 0.577 (205). UV−vis [1.0 × 10$^{-4}$ mol dm$^{-3}$; $\lambda_{max}$, nm ($\epsilon$, dm$^3$ mol$^{-1}$ cm$^{-1}$)]: 463 (4546), 588 (2393). $^1$H NMR ($\delta$, ppm; *J*, Hz): 12.71 (1H, s, NH); 7.85, 7.83 (1H, d, $J_{HH}$ 2.1; 2H, d, $J_{HH}$ 2.1; H5); 6.38, 6.36, 6.26 (1H, d, $J_{HH}$ 2.2; 1H, d, $J_{HH}$ 2.1; 1H, d, $J_{HH}$ 2.2; H4); 7.92, 7.54, 6.97 (2H, d, $J_{HH}$ 8.7; 2H, d, $J_{HH}$ 8.7; 2H, d, $J_{HH}$ 8.4; H$_o$); 6.95, 6.70, 6.34 (2H, d, $J_{HH}$ 8.7; 2H, d, $J_{HH}$ 8.7; 2H, d, $J_{HH}$ 8.4; H$_m$); 7.10, 6.32 (2H, d, $J_{HH}$ 8.7; 2H, d, $J_{HH}$ 8.4; C$_6$H$_4$); 3.85, 3.59, 3.48 (3H, s; 3H, s; 3H, s; CH$_3$O); 4.00 (5H, s, C$_5$H$_5$); 4.58, 4.33 (2H, t, $J_{HH}$ 1.2; 2H, t, $J_{HH}$ 1.2; C$_5$H$_4$). $^{13}$C NMR ($\delta$, ppm): 158.9, 157.8, 157.0 (C3); 137.2, 136.7, 136.3 (C5); 108.2, 108.0, 107.5 (C4); 160.1, 159.5, 159.4 (C$_p$); 131.5, 131.0, 130.7 (C$_o$); 126.2, 124.4, 124.0 (C$_\alpha$); 113.4, 112.9, 112.8 (C$_m$); 55.1, 55.0, 54.8 (CH$_3$O); 69.6 (C$_5$H$_5$); 84.3, 69.3, 69.2, 66.4, 66.0 (C$_5$H$_4$); 154.1, 137.8, 125.3, 121.9 (C$_6$H$_4$).

*Complex **2**.* Found: C, 54.51; H, 4.30; N, 11.54. Calcd for MoFeClBC$_{52}$H$_{46}$N$_{10}$O$_4$·CH$_2$Cl$_2$: C, 54.96; H, 4.19; N, 12.10. IR (cm$^{-1}$): $\nu$(NH) 3287; $\nu$(BH) 2495; $\nu$(NO) 1676. Mass spectrum (*m*/*z*, assignation): 1074 [M]$^+$, 1039 [M − Cl]$^+$, 658 [M − Cl − {NHC$_6$H$_4$[N═NC$_6$H$_4$-4-($\eta^5$-C$_5$H$_4$)Fe($\eta^5$-C$_5$H$_5$)]-4}]$^+$, 381 [H$_2$NC$_6$H$_4$[N═NC$_6$H$_4$-4-($\eta^5$-C$_5$H$_4$)Fe($\eta^5$-C$_5$H$_5$)]-4]. Cyclic voltammetry [$E_{1/2}$, V; ($\Delta E$, mV)]: −0.611 (88), 0.663 (78). UV−vis [1.9 × 10$^{-5}$ mol dm$^{-3}$; $\lambda_{max}$, nm ($\epsilon$, dm$^3$ mol$^{-1}$ cm$^{-1}$)]: 375 (10 730), 480 (14 753), 584 (sh). $^1$H NMR ($\delta$, ppm; *J*, Hz): 12.61 (1H, s, NH); 7.86, 7.84 (1H, d, $J_{HH}$ 2.3; 2H, d, $J_{HH}$ 2.4; H5); 6.38, 6.37, 6.26 (1H, d, $J_{HH}$ 2.1; 1H, d, $J_{HH}$ 2.1; 1H, d, $J_{HH}$ 2.2; H4); 7.87, 7.59, 6.95 (2H, d, $J_{HH}$ 8.8; 2H, d, $J_{HH}$ 8.4; 2H, d, $J_{HH}$ 8.5; H$_o$); 6.98, 6.68, 6.35 (2H, d, $J_{HH}$ 8.7; 2H, d, $J_{HH}$ 8.8; 2H, d, $J_{HH}$ 8.8; H$_m$); 7.82, 7.56 (2H, d, $J_{HH}$ 8.9; 2H, d, $J_{HH}$ 8.7; C$_6$H$_4$); 7.58, 6.51 (2H, d, $J_{HH}$ 8.6; 2H, d, $J_{HH}$ 8.8; C$_6$H$_4$); 3.87, 3.56, 3.45 (3H, s; 3H, s; 3H, s; CH$_3$O); 4.08 (5H, s, C$_5$H$_5$); 4.75, 4.42 (2H, t, $J_{HH}$ 1.8; 2H, t, $J_{HH}$ 1.8; C$_5$H$_4$); 5.30 (2H, s, CH$_2$Cl$_2$). $^{13}$C NMR ($\delta$, ppm): 157.8, 157.1, 157.0 (C3); 137.2, 136.8, 136.4 (C5); 108.4, 108.2, 107.7 (C4); 160.1, 159.6, 159.0 (C$_p$); 131.6, 130.9, 130.6 (C$_o$); 126.0, 124.2, 123.9 (C$_\alpha$); 113.4, 112.9, 112.8 (C$_m$); 57.2, 55.1, 54.8 (CH$_3$O); 69.8 (C$_5$H$_5$); 83.7, 69.7, 66.8, 66.7 (C$_5$H$_4$); 159.6, 149.8, 143.1, 136.9, 136.8, 126.3, 123.1, 122.9, 122.3 (C$_6$H$_4$).

*Complex **3**.* Found: C, 58.44; H, 4.62; N, 12.80. Calcd for MoFeClBC$_{53}$H$_{48}$N$_{10}$O$_4$: C, 58.55; H, 4.46; N, 12.88. IR (cm$^{-1}$): $\nu$(NH) 3279; $\nu$(BH) 2478; $\nu$(NO) 1675. Mass spectrum (*m*/*z*, assignation): 1088 [M]$^+$, 1053 [M − Cl]$^+$, 658 [M − Cl − {NHC$_6$H$_3$(3-CH$_3$)[N═NC$_6$H$_4$-4-($\eta^5$-C$_5$H$_4$)Fe($\eta^5$-C$_5$H$_5$)]-4}]$^+$. Cyclic voltammetry [$E_{1/2}$, V; ($\Delta E$, mV)]: −0.625 (126), 0.649 (88). UV−vis [9.2 × 10$^{-5}$ mol dm$^{-3}$; $\lambda_{max}$, nm ($\epsilon$, dm$^3$ mol$^{-1}$ cm$^{-1}$)]: 374 (13 155), 491 (13 395), 549 (sh). $^1$H NMR ($\delta$, ppm; *J*, Hz): 12.62 (1H, s, NH); 7.86, 7.82 (1H, d, $J_{HH}$ 2.1; 2H, d, $J_{HH}$ 2.1; H5); 6.37 (3H, br s, H4); 7.90, 7.59, 6.97 (2H, d, $J_{HH}$ 8.7; 2H, d, $J_{HH}$ 8.7; 2H, d, $J_{HH}$ 8.7; H$_o$); 6.99, 6.70, 6.38 (2H, d, $J_{HH}$ 8.7; 2H, d, $J_{HH}$ 8.7; 2H, d, $J_{HH}$ 8.7; H$_m$); 7.81, 7.59 (2H, d, $J_{HH}$ 8.4; 2H, d, $J_{HH}$ 8.4; C$_6$H$_4$); 7.36, 6.24, 6.17 (1H, d, $J_{HH}$ 8.7; 1H, d, $J_{HH}$ 1.8; 1H, dd, $J_{HH}$ 8.7, $J_{HH}$ 1.8; C$_6$H$_3$); 3.87, 3.59, 3.48 (3H, s; 3H, s; 3H, s; CH$_3$O); 4.07 (5H, s, C$_5$H$_5$); 4.74, 4.41 (2H, t, $J_{HH}$ 1.8; 2H, t, $J_{HH}$ 1.8; C$_5$H$_4$); 2.50 (3H, s, CH$_3$); $^{13}$C NMR ($\delta$, ppm): 157.8, 157.4, 157.0 (C3); 137.1, 136.7, 136.3 (C5); 108.4, 108.1, 107.7 (C4); 160.1, 159.5, 159.0 (C$_p$); 131.6, 130.9, 130.6 (C$_o$); 125.9, 124.1, 123.8 (C$_\alpha$); 113.4, 112.8, 112.7 (C$_m$); 55.1, 55.0, 54.7 (CH$_3$O); 69.8 (C$_5$H$_5$); 83.9, 69.6, 66.7, 66.7 (C$_5$H$_4$); 159.5, 151.3, 147.9, 142.8, 138.8, 126.3, 124.2, 122.9, 119.8, 115.3 (C$_6$H$_4$ and C$_6$H$_3$); 29.6 (CH$_3$).

*Complex **4**.* Found: C, 58.56; H, 4.80; N, 12.71. Calcd for MoFeClBC$_{54}$H$_{50}$N$_{10}$O$_4$: C, 58.89; H, 4.59; N, 12.70. IR (cm$^{-1}$): $\nu$(NH) 3281; $\nu$(BH) 2476; $\nu$(NO) 1675. Mass spectrum (*m*/*z*, assignation): 1102 [M]$^+$, 1067 [M − Cl]$^+$, 658 [M − Cl − {NHC$_6$H$_3$(3-CH$_3$)[N═NC$_6$H$_3$(3-CH$_3$)-4-($\eta^5$-C$_5$H$_4$)Fe($\eta^5$-C$_5$H$_5$)]-4}]$^+$, 409 [H$_2$NC$_6$H$_3$(3-CH$_3$)[N═NC$_6$H$_3$(3-CH$_3$)-4-($\eta^5$-C$_5$H$_4$)-Fe($\eta^5$-C$_5$H$_5$)]-4]. Cyclic voltammetry [$E_{1/2}$, V; ($\Delta E$, mV)]: −0.628 (141), 0.657 (83). UV−vis [1.1 × 10$^{-4}$ mol dm$^{-3}$; $\lambda_{max}$, nm ($\epsilon$, dm$^3$ mol$^{-1}$ cm$^{-1}$)]: 368 (13 028), 494 (17 615), 550 (sh). $^1$H NMR ($\delta$, ppm; *J*, Hz): 12.62 (1H, s, NH); 7.86, 7.83, 7.82 (1H, d, $J_{HH}$ 2.2; 1H, d, $J_{HH}$ 2.3; 1H, d, $J_{HH}$ 2.2; H5); 6.37 (3H, br s, H4); 7.89, 7.58, 6.96 (2H, d, $J_{HH}$ 8.8; 2H, d, $J_{HH}$ 8.7; 2H, d, $J_{HH}$ 8.6; H$_o$); 6.98, 6.71, 6.39 (2H, d, $J_{HH}$ 8.6; 2H, d, $J_{HH}$ 8.7; 2H, d, $J_{HH}$ 8.7; H$_m$); 7.80, 7.68, 7.66 (1H, d, $J_{HH}$ 8.1; 1H, d, $J_{HH}$ 8.1; 1H, s; C$_6$H$_3$); 7.34, 6.24, 6.16 (1H, d, $J_{HH}$ 8.7; 1H, d, $J_{HH}$ 2.2; 1H, dd, $J_{HH}$ 8.7, $J_{HH}$ 2.2; C$_6$H$_3$); 3.87, 3.60, 3.47 (3H, s; 3H, s; 3H, s; CH$_3$O); 4.16 (5H, s, C$_5$H$_5$); 4.59, 4.38 (2H, t, $J_{HH}$ 1.8; 2H, t, $J_{HH}$ 1.8; C$_5$H$_4$); 2.52, 2.51 (3H, s; 3H, s; CH$_3$). $^{13}$C NMR ($\delta$, ppm): 157.8, 157.4, 157.0 (C3); 137.1, 136.7, 136.3 (C5); 108.5, 108.2, 107.7 (C4); 160.1, 159.6, 159.0 (C$_p$); 131.6, 131.0, 130.7 (C$_o$); 126.0, 124.1, 123.9 (C$_\alpha$); 113.4, 112.8, 112.7 (C$_m$); 55.1, 55.0, 54.7 (CH$_3$O); 69.6 (C$_5$H$_5$); 86.0, 69.9, 69.8, 68.5 (C$_5$H$_4$); 159.5, 151.1, 148.0, 141.0, 138.8, 136.2, 130.8, 125.6, 124.2, 119.8, 119.2, 115.3 (C$_6$H$_3$); 21.5, 17.3 (CH$_3$).

*Complex **5**.* Found: C, 57.70; H, 4.56; N, 9.53. Calcd for MoFeClBC$_{46}$H$_{41}$N$_7$O$_5$: C, 56.96; H, 4.27; N, 10.11. IR (cm$^{-1}$): $\nu$(BH) 2480; $\nu$(NO) 1694. Mass spectrum (*m*/*z*, assignation): 971 [M]$^+$, 936 [M − Cl]$^+$, 657 [M − Cl − {OC$_6$H$_4$-4-($\eta^5$-C$_5$H$_4$)Fe($\eta^5$-C$_5$H$_5$)}]$^+$, 278 [HOC$_6$H$_4$-4-($\eta^5$-C$_5$H$_4$)Fe($\eta^5$-C$_5$H$_5$)]. Cyclic voltammetry [$E_{1/2}$, V; ($\Delta E$, mV)]: −0.386 (156), 0.598 (142). UV−vis [1.0 × 10$^{-4}$ mol dm$^{-3}$; $\lambda_{max}$, nm ($\epsilon$, dm$^3$ mol$^{-1}$ cm$^{-1}$)]: 505 (4840), 780 (2405). $^1$H NMR ($\delta$, ppm; *J*, Hz): 7.95, 7.90, 7.77 (1H, d, $J_{HH}$ 2.1; 1H, d, $J_{HH}$ 2.4; 1H, d, $J_{HH}$ 2.4; H5); 6.41, 6.33, 6.28 (1H, d, $J_{HH}$ 2.4; 1H, d, $J_{HH}$ 2.4; 1H, d, $J_{HH}$ 2.1; H4); 7.47, 7.34, 7.02 (2H, d, $J_{HH}$ 9.0; 2H, d, $J_{HH}$ 9.0; 2H, d, $J_{HH}$ 8.7; H$_o$); 6.88, 6.49, 6.32 (2H, d, $J_{HH}$ 8.7; 2H, d, $J_{HH}$ 8.7; 2H, d, $J_{HH}$ 9.0; H$_m$); 7.21, 6.49 (2H, d, $J_{HH}$ 8.7; 2H, d, $J_{HH}$ 8.7; C$_6$H$_4$); 3.82, 3.53, 3.46 (3H, s; 3H, s; 3H, s; CH$_3$O); 4.07 (5H, s, C$_5$H$_5$); 4.60, 4.31 (2H, t, $J_{HH}$ 1.8; 2H, t, $J_{HH}$ 1.8; C$_5$H$_4$). $^{13}$C NMR ($\delta$, ppm): 158.6, 158.1, 158.0 (C3); 137.7, 136.6, 135.6 (C5); 108.3, 107.9, 107.5 (C4); 159.8, 159.6, 159.0 (C$_p$); 131.3, 130.5, 130.4 (C$_o$); 125.9, 125.4, 123.6 (C$_\alpha$); 113.0, 112.9, 112.2 (C$_m$); 55.0, 54.9, 54.8 (CH$_3$O); 69.8 (C$_5$H$_5$); 85.7, 69.2, 69.1, 66.4, 66.1 (C$_5$H$_4$); 167.5, 135.3, 125.6, 117.9 (C$_6$H$_4$).

*Complex **6**.* Found: C, 60.64; H, 4.24; N, 9.82. Calcd for MoFeClBC$_{54}$H$_{48}$N$_8$O$_4$: C, 60.55; H, 4.53; N, 10.46. IR (cm$^{-1}$): $\nu$(NH) 3277; $\nu$(BH) 2477; $\nu$(NO) 1668. Mass spectrum (*m*/*z*, assignation): 1072 [M]$^+$, 1037 [M − Cl]$^+$, 658 [M − Cl − {NHC$_6$H$_4$[CH═CHC$_6$H$_4$-4-($\eta^5$-C$_5$H$_4$)Fe($\eta^5$-C$_5$H$_5$)]-4}]$^+$. Cyclic voltammetry [$E_{1/2}$, V; ($\Delta E$, mV)]: −0.766 (88), 0.610 (78).

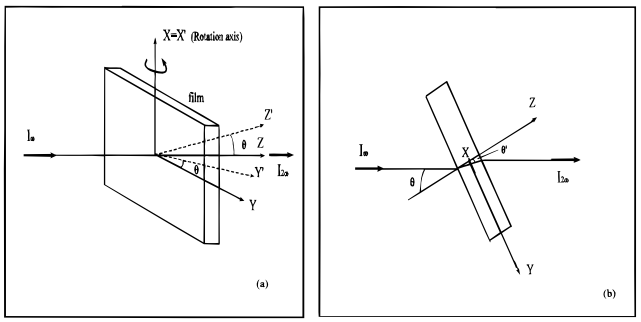


**Figure 3.** Experimental geometry. (a) Three-dimensional perspective and (b) projection on a plane perpendicular to the rotation (*X*) axis. *X*′, *Y*′, *Z*′ stand for the film axes, and *X*, *Y*, and *Z* refer to the laboratory axes.

UV−vis [$9.4 \times 10^{-5}$ mol dm$^{-3}$; $\lambda_{max}$, nm ($\epsilon$, dm$^3$ mol$^{-1}$ cm$^{-1}$)]: 345 (20 996), 528 (11 664). $^1$H NMR ($\delta$, ppm; *J*, Hz): 12.65 (1H, s, NH); 7.86, 7.83 (1H, d, $J_{HH}$ 2.1; 2H, br; H5); 6.36, 6.26 (2H, br; 1H, d, $J_{HH}$ 2.1; H4); 7.89, 7.57, 6.95 (2H, d, $J_{HH}$ 8.7; 2H, d, $J_{HH}$ 8.7; 2H, d, $J_{HH}$ 8.7; $H_o$); 6.97, 6.68, 6.35 (2H, d, $J_{HH}$ 8.7; 2H, d, $J_{HH}$ 8.7; 2H, d, $J_{HH}$ 8.7; $H_m$); 7.00 (2H, s, CH═CH); 7.15, 6.35 (2H, d, $J_{HH}$ 8.4; 2H, d, $J_{HH}$ 8.4; $C_6H_4$); 7.47, 7.42 (4H, AB system, $J_{HH}$ 8.1; $C_6H_4$); 3.86, 3.56, 3.53 (3H, s; 3H, s; 3H, s; $CH_3O$); 4.06 (5H, s, $C_5H_5$); 4.67, 4.35 (2H, t, $J_{HH}$ 1.8; 2H, t, $J_{HH}$ 1.8; $C_5H_4$). $^{13}$C NMR ($\delta$, ppm): 157.8, 157.0, 155.3 (C3); 137.1, 136.7, 136.3 (C5); 108.3, 108.0, 107.5 (C4); 160.0, 159.5, 158.9 ($C_p$); 131.5, 130.9, 130.6 ($C_o$); 127.0, 124.2, 123.9 ($C_\alpha$); 113.4, 112.8, 112.8 ($C_m$); 55.1, 55.0, 54.8 ($CH_3O$); 69.5 ($C_5H_5$); 84.7, 69.0, 66.3 ($C_5H_4$); 159.4, 139.0, 135.1, 134.7, 128.3, 126.4, 126.2, 126.1, 122.1 ($C_6H_4$).

**2.2. Preparation of Ordered Thin Films.** Films were prepared from chlorobenzene solutions containing the host polymer PMMA and the organometallic compound. For all systems, the weights of these two species in the solution were in a ratio of 10:1, respectively. The concentrations of organometallic molecules in the films, determined from the optical absorption spectra, ranged from $6 \times 10^{19}$ to $18 \times 10^{19}$ cm$^{-3}$. The film thicknesses were between 0.6 and 2 $\mu$m, as measured with a standard profilometer. Molecular ordering was achieved by corona poling with sample temperature 65 °C, poling voltage 6 kV, and poling time 30 min.

**2.3. Dipole Moment Measurements.** The ground-state dipole moments, $\mu^{(0)}$, of molecules **1**, **2**, and **4** were determined by capacitance measurements following the classical Guggenheim method.[16]

**2.4. Optical Techniques.** Optical absorption spectra for the spin-coated films were measured in the wavelength range of 300−800 nm with a Hitachi U-3501 spectrophotometer. The $\chi^{(2)}$ susceptibilities have been determined by the Maker fringes technique[17−19] using an *x*-cut $LiNbO_3$ plate as a reference ($\chi^{(2)}_{33} = 1.96 \times 10^{-7}$ esu). Fundamental light from a Q-switched Nd:YAG laser (10-ns pulse duration and 10-Hz repetition rate) operating at 1.064 $\mu$m was incident along the *z* direction (see Figure 3). The second-harmonic light signal was detected with a photomultiplier, averaged with a boxcar integrator, and stored in a computer.

## 3. Results

**3.1. Optical Spectra.** The optical absorption spectra of compounds **1**, **2**, and **5**−**7** in the spin-coated films prior to poling are shown in Figure 4. This information is very relevant for an adequate discussion of the SHG results. Spectra for the compounds in dichloromethane solutions are nearly identical to those found in films.

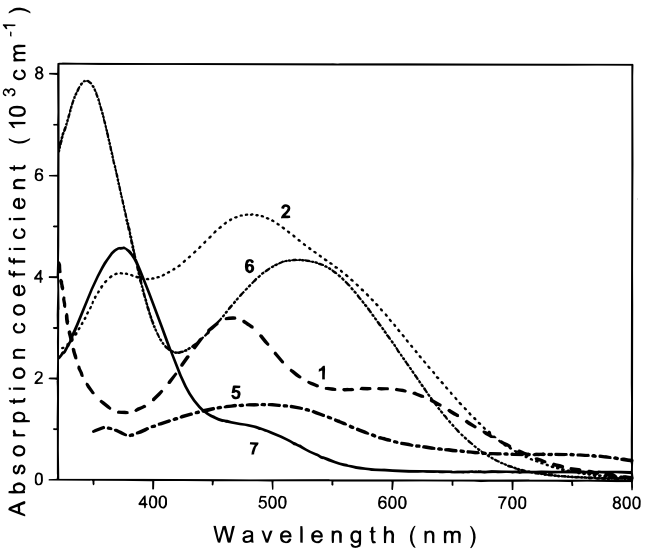


**Figure 4.** Optical absorption spectra for the films containing compounds **1**, **2**, and **5**−**7**. Film thicknesses are given in Table 2.

Compound **7** with a ferrocenyl group bonded to the $O_2N-C_6H_4-CH═CH-C_6H_4$- system shows two absorption bands at 374 and 495 nm, within the range observed for related nitroferrocenyl derivatives.[20] On the basis of previous data,[21] these bands were assigned to CT transitions from the metal to the nonbonding or antibonding orbitals of the cyclopentadienyl ligand. The electronic spectra of bimetallic species **1**−**6** show also two main absorption bands (see section 2.1(a)). For compounds **2**−**4** and **6**, one of them appears in the ultraviolet region and the other in the visible range. For compounds **1** and **5**, both bands appear in the visible region. The $\epsilon$ values are consistent with their assignation to CT transitions, in which the ferrocenyl and molybdenum groups should be involved. However, the precise nature of these bands has not been established.

For comparative purposes, three sets of compounds were considered. The first one corresponds to compounds **1** and **5**, from which the influence of the Y-coordinating group can be inferred. The electronic spectral data indicate a higher energy for the CT bands when the NH ligands are involved in the molybdenum center (Figure 4). The second set includes compounds **2**−**4**, whose differences arise from the substituents in the bridge. No influence from the methyl substituents has been observed. The influence of the $-C_6H_4-N═N-C_6H_4-$ or $-C_6H_4-CH═CH-C_6H_4-$ bridging systems was inferred from a comparison between compounds **2** and **6** (third set) (Figure 4). Significant variations of the intensity (not position) of the bands are induced depending on the presence of either a N═N or a C═C linking group in the bridging system. Additionally, the spectra of complexes **6** and **7** (Figure 4) having the ferrocenyl donor group $Fc-C_6H_4-CH═CH-C_6H_4-$ bonded to the different acceptor groups, $[Mo(Tp^{An})(NO)(Cl)(Y)]$ or $NO_2$, respectively, showed significant differences in the intensity of the lowest energy band. So, the nitro derivative, **7**, presents an absorption band at 495 nm approximately 4 times less intense than that at 528 nm for the related bimetallic derivative, **6**.

The optical absorption coefficients, $\alpha$, for the low-energy visible bands of our compounds are not significantly modified by poling. The data of the relative change $\Delta\alpha/\alpha$ for three representative compounds, **1**, **2**, and **7**, are shown as short segments in Figure 5, assuming that $p = \mu E_p/kT$ is in the range of 2−3. This range is expected from the measured $\mu^{(0)}$ values (∼10 D) and the fields, $E_p$, of 2−4 MV/cm achieved by corona poling. In fact, fields of about 3 MV/cm have been estimated

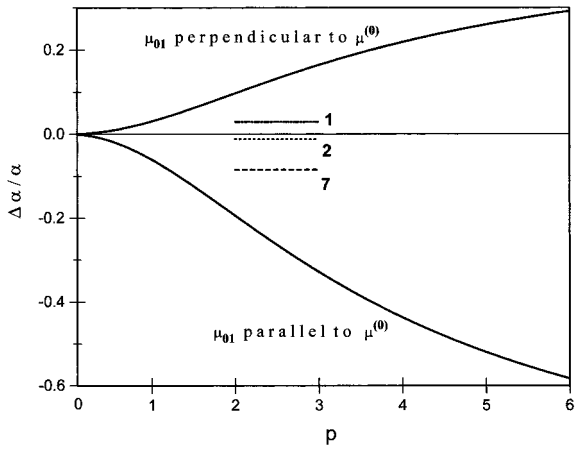


**Figure 5.** Theoretical predictions for the relative change in absorption induced by an applied field when $\mu_{01}$ is either parallel or perpendicular to $\mu^{(0)}$. The experimental data for compounds **1**, **2**, and **7** are indicated by short segments.

in similar PMMA spin-coated films prepared by us and containing quasi-axial molecules (SubPcs). In principle, for a transition dipole moment ($\mu_{01}$) parallel to the permanent (static) dipole moment [$\mu^{(0)}$], poling should induce a clear decrease in the absorption coefficient, as illustrated in Figure 5. The expected decrease $\Delta\alpha/\alpha$ has been calculated as a function of poling field through the expression[22,23]

$$\left(\frac{\Delta\alpha}{\alpha}\right)_{\parallel} = \frac{\alpha(p) - \alpha(0)}{\alpha(0)} = \frac{3}{p}\coth(p) - \frac{3}{p^2} - 1 \qquad (1)$$

and assuming that thermal orientational equilibrium has been achieved. Relative decreases of $\Delta\alpha/\alpha > 25\%$ are expected and have been measured[22−24] for molecules with moderate dipole moments under poling voltages of several kilovolts. Although the organometallic molecules investigated in this work have large dipole moments of around 10 D and therefore $p$ should be between 2 and 3, such large changes have not been observed. Therefore, our experimental results suggest that the two dipole moments (transition and permanent) are not aligned but are tilted to each other. In other words, the transition moment should have both parallel and perpendicular components to the effective molecular axis defined by the permanent moment. For a transition moment, $\mu_{01}$, perpendicular to $\mu^{(0)}$, the relative change in the absorption coefficient, $\Delta\alpha/\alpha$, has been calculated, and it is given by

$$\left(\frac{\Delta\alpha}{\alpha}\right)_{\perp} = \frac{1}{2} - \frac{3}{2p}\coth(p) + \frac{3}{2p^2} \qquad (2)$$

The absorption coefficient increases with the poling field as shown in Figure 5. Our experimental data lie below the two theoretical curves in the figure, confirming the occurrence of both parallel and perpendicular contributions to the transition moment. The perpendicular component may be associated with transitions involving electronic states with mixed metal−ligand orbitals and $\pi$-conjugated orbitals of the bridge. In fact, the measured $\Delta\alpha/\alpha$ is slightly positive for compounds **1** and **5** (which contain the [Mo(Tp$^{An}$)(NO)(Cl)(Y)] acceptor group) and is significantly negative for compound **7** (which has the better aligned nitro group). Moreover, the value is small and positive for the shorter compound **1**, but for the similar but longer compound **2**, it is slightly negative. These results are consistent with the proposed model because the expected contribution of the perpendicular component to $\Delta\alpha/\alpha$ should be higher for **1**.

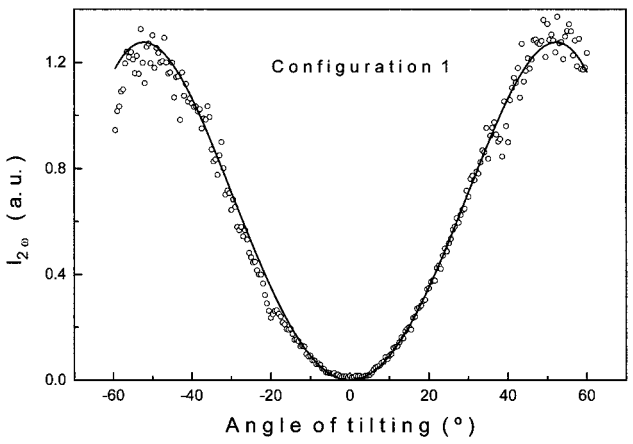


**Figure 6.** Maker fringes data for a film with **2** using configuration 1. The solid line corresponds to the best fit to the theoretical expression.

**TABLE 1: Fundamental and Harmonic Polarization Configurations for the SHG Experiments**

| configuration | $E_\omega$ | $E_{2\omega}$ |
|---|---|---|
| 1 | *X* | *Y* |
| 2 | *Y* | *Y* |
| 3 | 45° | *X* |

Finally, the parallel and perpendicular components of the transition moment can be calculated from the data in Figure 5. From them, the tilting angle between the two moments has been estimated, and it varies from 43° for **7** to 59° for **1**. Further confirmation of the occurrence of the perpendicular components is provided by the SHG experiment to be discussed in section 3.2.

**3.2. SHG Results.** SHG experiments were carried out as a function of the sample's rotation angle around an axis (*X*) in the film plane, as schematically illustrated in Figure 3. Three different light polarization configurations were used and are indicated in Table 1. As an example, typical results for the SHG yield in configuration 1 are shown in Figure 6.

The $\chi^{(2)}$ values were determined from the analysis of the Maker fringes following the procedure given in refs 17−19. The equation giving the effective second-harmonic intensity as a function of the rotation angle $\theta$ can be expressed as[18,25]

$$I_{2\omega}(\theta) = \frac{64\pi^3\omega^2\chi_{\mathrm{eff}}{}^2 I_0{}^2 T}{n_\omega{}^2 n_{2\omega} c^3} \times \exp[(-\alpha_{2\omega}L)/(2\cos\theta')]\frac{\cosh\left(\frac{\alpha_{2\omega}L}{2\cos\theta'}\right) - \cos\left(\frac{\Delta kL}{\cos\theta'}\right)}{\frac{\alpha_{2\omega}{}^2}{4} + \Delta k^2} \qquad (3)$$

where $I_0$ is the incident fundamental intensity, $L$ the film thickness, and $T$ an overall transmission factor accounting for both fundamental and harmonic reflections at the various boundaries. $\chi_{\mathrm{eff}}$ is the effective susceptibility corresponding to the polarization configuration used in the experiment. Finally, $\theta$ and $\theta'$ are the angles formed by the normal to the film with the fundamental wavevector, outside and inside the film, respectively (see Figure 3). Other symbols have the usual meanings. The absolute indexes $n_\omega$ and $n_{2\omega}$ were taken as those for PMMA. On the other hand, the index mismatch $\Delta n = n_{2\omega} - n_\omega$ was left as a fitting parameter starting from the value for PMMA. The best fitting was obtained for $\Delta n = 0.06$ that corresponds to a coherence length larger than the film thickness.

**TABLE 2: Susceptibility Values, Molecular Concentrations and Film Thicknesses[a]**

| sample | $N$ ($10^{19}$ cm$^{-3}$) | $\chi^{(2)}_{31}$ ($10^{-9}$ esu)[a] | $\chi^{(2)}_{15}$ ($10^{-9}$ esu)[a] | $\chi^{(2)}_{33}$ ($10^{-9}$ esu)[a] | thickness ($\mu$m) |
|---|---|---|---|---|---|
| 1 | 18 | 1.3 | −0.5 | 0.4 | 1.8 |
| 2 | 7.1 | 1.9 | −0.7 | 0.6 | 1.65 |
| 3 | 6.9 | 1.4 | −0.4 | 0.4 | 1.7 |
| 4 | 7.2 | 1.5 | −0.4 | 0.7 | 1.5 |
| 5 | 13 | very low | very low | very low | 1.3 |
| 6 | 16 | 2.4 | −1.0 | 0.7 | 1.5 |
| 7 | 6 | 6.6 | −4.2 | −2.4 | 1.4 |

[a] 1 esu = $4.19 \times 10^8$ pm/V.

Equation 3, which takes into account the absorption coefficient ($\alpha_{2\omega}$) at the harmonic frequency, neglects the second derivative of the field amplitude in the wave equation caused by attenuation (slowly varying approximation). However, this procedure is reasonable because the error induced by this approximation is ≤12% for the $\alpha_{2\omega}$ values measured in our samples.

The effective susceptibilities for the different polarization configurations[18] are

Configuration 1

$$\chi_{\text{eff}} = -\chi^{(2)}_{31} \sin\theta' = -\chi^{(2)}_{31}\frac{\sin\theta}{n_\omega} \tag{4a}$$

Configuration 2

$$\chi_{\text{eff}} = -[(2\chi^{(2)}_{15} + \chi^{(2)}_{31})\cos^2\theta' + \chi^{(2)}_{33}\sin^2\theta']\sin\theta' \tag{4b}$$

Configuration 3

$$\chi_{\text{eff}} = -\chi^{(2)}_{15} \sin\theta' = -\chi^{(2)}_{15}\frac{\sin\theta}{n_\omega} \tag{4c}$$

The values obtained for the three nonzero components of the $\boldsymbol{\chi}^{(2)}$ tensor are listed in Table 2. On the basis of the the fitting procedure, absolute magnitudes and relative signs for all susceptibility components are well-determined. In Table 2, the sign of $\chi^{(2)}_{31}$ has been arbitrarily chosen as positive.

## 4. Discussion and Conclusions

One first sees from the reported data that $\chi^{(2)}_{31}$ is the largest component and that Kleinman symmetry is not obeyed. These are relevant results, indicating that our compounds cannot be considered linear (one-dimensional) molecules in which the only nonzero component of the quadratic hyperpolarizability tensor is $\beta_{33} = \beta_{zzz}$ and the relation $\chi^{(2)}_{33} = 3\chi^{(2)}_{31}$ should be expected. The departure from the expectation for linear molecules again suggests that the transition dipole moment of the relevant low-energy optical transition is not parallel to the permanent moment, which is presumably aligned along the effective molecular axis connecting the donor and acceptor moieties. In fact, it has been inferred from a two-level model and experimentally confirmed that the tilting between the two moments should give rise to off-diagonal components of the $\boldsymbol{\beta}$ tensor.[26,27] To support this conclusion and confirm the occurrence of such off-diagonal components, the $\beta_{ij}$ tensor has been estimated from $\chi^{(2)}_{ij}$ under the assumption of $C_{\infty v}$ symmetry for the molecules and thermal equilibrium under poling. The equation which relates the two tensors was derived by Kielich:[13]

$$\chi^{(2)}_{15} = (N/2)f_{2\omega}f_\omega{}^2\{[L_1(p) - L_3(p)]\beta_{33} + [L_3(p) - L_1(p)]\beta_{31} + [2L_3(p)]\beta_{15}\}$$

$$\chi^{(2)}_{31} = (N/2)f_{2\omega}f_\omega{}^2\{[L_1(p) - L_3(p)]\beta_{33} + [L_3(p) + L_1(p)]\beta_{31} + 2[L_3(p) - L_1(p)]\beta_{15}\}$$

$$\chi^{(2)}_{33} = Nf_{2\omega}f_\omega{}^2\{[L_3(p)]\beta_{33} + [L_1(p) - L_3(p)]\beta_{31} + 2[L_1(p) - L_3(p)]\beta_{15}\} \tag{5}$$

where $L_n$ stands for the $n$th-order Langevin function and $f_\omega$ and $f_{2\omega}$ are the appropriate Lorentz local field factors ($f_\omega = (n_\omega{}^2 + 2)/3$).

The values obtained for the three nonzero components $\beta_{31}$, $\beta_{15}$, and $\beta_{33}$ for molecules **1**, **2**, and **4** are given in Table 3 for two reasonable values of the poling field corresponding to $p = 2$ and $p = 3$. Although values are slightly different depending on $p$, the main trend is maintained; i.e., $\beta_{31}$ is the largest component and the ratio $\beta_{31}/\beta_{33}$ is not appreciably affected by $p$. The same qualitative behavior is observed even for poling fields outside the above range. The occurrence of large off-diagonal components $\beta_{zxx} = \beta_{31}$ and $\beta_{zxz} = \beta_{15}$ of the $\boldsymbol{\beta}$ tensor has been theoretically predicted[26] within a two-level approximation for CT bands having a transition moment perpendicular to the molecular axis. This prediction has been experimentally confirmed on several two-dimensional complexes.[27] Moreover, according to this simple two-level model, deviations from the Kleinman symmetry condition when either $\omega$ or $2\omega$ (or both) is near resonance are expected[26] and have been observed[27] because of the different dispersion factors involved in the $\beta_{31}$ and $\beta_{15}$ components. Our experimental results show these features and so could be explained with such a model. This interpretation is consistent with the data described in section 3.1 on the effect of poling voltage on the low-energy bands, mostly responsible for the NLO response at $\lambda = 1.064$ $\mu$m. To the best of our knowledge, this work is the first one where such high off-diagonal components of $\boldsymbol{\beta}$ have been observed for quasi-linear molecules, i.e., having a main effective axis. It can then be concluded that the measurements of the three tensor components of the susceptibility and a detailed knowledge of the electronic spectra are key elements for a good understanding of the SHG response.

Other main conclusions inferred from our comparative study are as follows:

(a) $\chi^{(2)}$ values are, in general, competitive with those measured for a few organometallic crystals.[28,29] Because of the relatively high absorption at the harmonic frequency, $\chi^{(2)}$ values are resonantly enhanced. For $\chi^{(2)}_{33}$, the enhancement factor has been estimated to be around 3 from a simple two-level model. However, **5** (which contains the Y = O group) did not show any appreciable SHG response, in agreement with previous work.[9,30]

(b) Although the susceptibility values are similar for **1**−**4**, the much higher concentration for **1** allows us to conclude that $\chi^{(2)}$ values are considerably enhanced when the donor and acceptor metal groups are connected through the diarylazoamide (NH−$C_6H_4$−N═N−$C_6H_4$) instead of the anilide (NH−$C_6H_4$) bridge. This behavior is in accordance with previous qualitative results obtained by the Kurtz method[9,10] and should be related to the increase in conjugation length provided by the diarylazo group.

(c) The incorporation of methyl substituents (R, R′) at the connecting diarylazoamide [NH−$C_6H_3$R−N═N−$C_6H_3$R′(R = R′= H; R = $CH_3$, R′= H; R = R′ = $CH_3$)] bridge does not

**TABLE 3: Estimated Values for the Quadratic Hyperpolarizabilities Corresponding to $p = 2$ and $p = 3$ and Related Electric Poling Field**

| compound | $p$ | $E_p$ (MV/cm) | $\beta_{31}$ ($10^{-30}$ esu) | $\beta_{15}$ ($10^{-30}$ esu) | $\beta_{33}$ ($10^{-30}$ esu) |
|---|---|---|---|---|---|
| 1 | 2 | 2.6 | 4.6 | −2.1 | 1.9 |
| | 3 | 3.9 | 3.8 | −1.5 | 1.3 |
| 2 | 2 | 2.7 | 17.3 | −7.2 | 7.8 |
| | 3 | 4.1 | 14.3 | −5.3 | 5.3 |
| 4 | 2 | 2.8 | 13.6 | −4.7 | 7.8 |
| | 3 | 4.2 | 11.2 | −3.4 | 5.6 |

appreciably modify $\chi^{(2)}$ in accordance with the close similarity of the absorption spectra for compounds **2**−**4**. However, this result is at variance with those reported using the Kurtz method for a related compound having the $Tp^{Me2}$ ligand. In this case, the attachment of one methyl substituent produced a strong increase in the Kurtz value.[9] Therefore, this enhancement should be attributed to a more favorable molecular packing but not to the intrinsic molecular response.

(d) From a comparison between **2** and **6** (after normalization of the $\chi^{(2)}$ values to the same molecular concentration), it appears that the N═N group at the bridge is more effective for SHG than the C═C group. This may be due to the higher polarizability of the N═N bond than that of C═C.

(e) Through comparison of the results between the two stilbenyl derivatives, **6** and **7**, it can be concluded that the nitro group behaves as a much stronger acceptor than the [Mo(Tp$^{An}$)(NO)(Cl)(Y)] group, leading to susceptibility values around 3 times higher for the 4-nitro-4′-ferrocenylstilbene (**7**) compound. The measured susceptibility (out of resonance) is very significant and similar to the off-resonant susceptibilities reported for guest−host PMMA systems containing the well-known dye DR1. In fact, values in the range of (14−48) × $10^{-9}$ esu[18,31,32] have been obtained in these systems but for molecular concentrations about 4 times higher than that used in our experiment. It is very noteworthy that our compound **7** presents very high $\chi^{(2)}$ values in spite of the fact that the Kurtz value is 1 with regard to urea.[20] This indicates that although the molecular response is large, the crystallization process strongly reduces it. In fact, an antiparallel ordering of the dipole moments may be expected in the crystals because of the very different sizes of the acceptor ($NO_2$) and donor (ferrocenyl) groups.[9]

## 5. Relaxation Behavior

To provide a more complete assessment of the films containing organometallic compounds, the relaxation behavior of the second-harmonic susceptibility has been investigated at room temperature. This information is relevant when practical applications are being considered. Experiments have been carried out on two representative molecules of the set, **2** and **7**. The comparison between the results for these two molecules will permit us to evaluate the role of size on relaxation kinetics. Results for the highest $\chi^{(2)}_{31}$ component are plotted in Figure 7. For the two molecules, the relaxation data very approximately follow a biexponential decay[33] including fast and slow stages. As illustrated in Figure 7, they can also be well fitted with the Williams−Watts−Kohlrausch $\{\chi = \chi_\infty + \Delta\chi \exp[-(t/\tau)^\beta]\}$[34,35] law, where $\chi_\infty$ stands for the long term ($t = \infty$) value of the susceptibility, $\tau$ is a relaxation time, and $\beta$ is a relaxation exponent. This relaxation kinetics has been observed for many polymeric systems and appears to have a wide range of validity. Fitting parameters for our data in Figure 7 are $\chi_\infty = 0.7$, $\beta = 0.48$, $\tau = 125$ min (**2**) and $\chi_\infty = 0.65$, $\beta = 0.45$, $\tau = 49$ min (**7**). One sees from the figure that **7** relaxes more rapidly than **2**. Because the glass transition temperature is expected to be roughly the same in both films, this effect may be associated to the smaller size of **7**, which permits a less hindered motion inside the PMMA host. As inferred from Figure 7, the fast relaxation stage exhausts after about 10 h at room temperature, and a rather stable level at around 50% of the initial one is reached. For comparison, the parameters measured[34] for DR1 dye into PMMA are $\beta = 0.181$ and $\tau = 467$ min, implying a much lower relaxation rate.

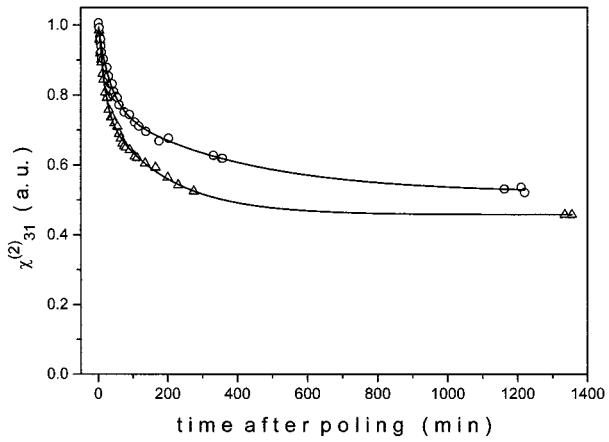


**Figure 7.** Room temperature decay relaxation of the susceptibility for **2** (circles) and **7** (triangles). The best fitting to a William−Watts−Kohlrausch law is shown by the solid lines.

## 6. Summary

In summary, the SHG capabilities of poled PMMA films containing donor−acceptor organobimetallic molecules have been evaluated. All three nonzero components of the $\boldsymbol{\chi}^{(2)}$ tensor have been determined. Significant $\chi^{(2)}_{ij}$ values have been achieved for most compounds. The highest component is $\chi^{(2)}_{31}$ at variance with the situation expected for linear (one-dimensional) molecules where $\chi^{(2)}_{33} = 3\chi^{(2)}_{31}$. Moreover, Kleinman symmetry is not obeyed, i.e., $\chi^{(2)}_{31} \neq \chi^{(2)}_{15}$. These peculiar features have been related to low-energy CT transitions whose dipole moments have a component which is perpendicular to the permanent moment and so to the effective molecular axis. In accordance with this conclusion, the estimated hyperpolarizability tensor presents three nonzero components ($\beta_{33}$, $\beta_{31}$, and $\beta_{15}$), assuming $C_{\infty v}$ symmetry. Moreover, the estimated off-diagonal component $\beta_{31}$ has been shown to be dominant. On the other hand, definite trends for the role of the bridging structure and the effect of the substituents on the SHG susceptibilities have clearly been established. In many cases, they differ from those derived from Kurtz data. Moreover, the nitro group behaves as a much better acceptor than the [Mo(Tp$^{An}$)(NO)(Cl)(Y)] acceptor group in compounds having the same ferrocenyl donor group and polarizable bridging system, and remarkable $\chi^{(2)}_{ij}$ susceptibilities have been obtained for the 4-nitro-4′-ferrocenylstilbene compound (**7**). Finally, the thin-film strategy, because of its technological relevance, should be actively pursued to provide a better assessment of the capabilities of organometallic compounds for NLO.

**Acknowledgment.** We acknowledge financial support from Projects PB950370 and TIC 96-0668 and European Contract CI1*-CT94-0039.

## References and Notes

(1) Chemla, D. S., Zyss, J., Eds. *Nonlinear Optical Properties of Molecules and Crystals*; Academic Press: Orlando, FL, 1987.

(2) Prasad, P. N., Williams, D. J., Eds. *Introduction to Nonlinear Optical Effects in Molecules and Polymers*; Wiley: New York, 1991.

(3) Nalwa, H. S., Miyata, S., Eds. *Nonlinear Optics of Organic Molecules and Polymers*; CRC Press: Boca Raton, FL, 1997.

(4) Nalwa, H. S. *Appl. Organomet. Chem.* **1991**, *5*, 349.

(5) Long, N. J. *Angew. Chem., Int. Ed. Engl*. **1995**, *34*, 21.

(6) Green, M. L.; Marder, S. R.; Thompson, M. E.; Brandy, J. A.; Bloor, D.; Kolinsky, P. V.; Jones, R. J. *Nature* **1987**, *330*, 360.

(7) Kurtz, S. K.; Perry, T. T. *J. Appl. Phys.* **1968**, *39*, 3798.

(8) McCleverty, J. A. *Polyhedron* **1989**, *8*, 1169.

(9) Coe, B. J.; Foulon, J. D.; Hamor, T. A.; Jones, C. J.; McCleverty, J. A.; Bloor, D.; Cross, G. H.; Axon, T. L. *J. Chem. Soc., Dalton Trans*. **1994**, 3427.

(10) Coe, B. J.; Jones, C. J.; McCleverty, J. A.; Bloor, D.; Kolinsky, P. V.; Jones, R. J. *Polyhedron* **1994**, *13*, 2107.

(11) Coe, B. J.; Hamor, T. A.; Jones, C. J.; McCleverty, J. A.; Bloor, D.; Cross, G. H.; Axon, T. L. *J. Chem. Soc., Dalton Trans.* **1995**, 673.

(12) Comizzoli, R. B. *J. Electrochem. Soc.* **1987**, *134*, 424.

(13) Kielich, S. *IEEE J. Quantum Electron*. **1969**, *5*, 562.

(14) Broadhead, G. D.; Pauson, P. L. *J. Chem. Soc.* **1955**, 367.

(15) Cano, M.; Heras, J. V.; Monge, A.; Gutiérrez, E.; Jones, C. J.; McWhinnie, S. L. W.; McCleverty, J. A. *J. Chem. Soc., Dalton Trans.* **1992**, 2435.

(16) Guggenheim, E. A. *Trans. Faraday Soc.* **1949**, *45*, 714.

(17) Eich, M.; Sen, A.; Looser, H.; Bjorklund, G. C.; Swalen, J. D.; Tweig, R.; Yoon, D. Y. *J. Appl. Phys.* **1989**, *66*, 2559.

(18) Hayden, L. M.; Sauter, G. F.; Ore, F. R.; Pasillas, P. L.; Hoover, J. M.; Lindsay, G. A.; Henry, R. A. *J. Appl. Phys.* **1990**, *68*, 456.

(19) Rojo, G.; Hierro, A.; Diaz-García, M. A.; Agulló-López, F.; del Rey, B.; Sastre, A., Torres, T. *Appl. Phys. Lett.* **1997**, *70*, 1802.

(20) Coe, B. J.; Jones, C. J.; McCleverty, J. A.; Bloor, D.; Cross, G. H. *J. Organomet. Chem.* **1994**, *464*, 225.

(21) Rosemblum, M.; Santer, J. O.; Howells, W. G. *J. Am. Chem. Soc.* **1963**, *85*, 1450.

(22) Mortazavi, M. A.; Knoesen, A.; Towel, S. T.; Higgings, B. G.; Dienes, A. *J. Opt. Soc. Am.* **1989**, *B6*, 733.

(23) Martinez, D. R.; Koch, K.; Ratsorong, F. K.; Carlinge, G. O. *J. Appl. Phys.* **1994**, *75*, 4273.

(24) Mandal, B. K.; Chen, Y. M.; Lee, J. Y.; Kumar, J.; Tripathy, S. *Appl. Phys. Lett.* **1991**, *58*, 2459.

(25) Zyss, J.; Chemla, D. S. In *Nonlinear Optical Properties of Molecules and Crystals*; Academic Press: Orlando, FL, 1987; Vol. 1, p 23.

(26) Wortmann, R.; Krämer, P.; Glania, C.; Lebus, S.; Detzer, N. *Chem. Phys.* **1993**, *173*, 99.

(27) (a) Wolf, J. J.; Langle, D.; Hillenbrand, D.; Wortmann, R.; Matschiner, R.; Glania, C.; Kramer, P. *Adv. Mater. (Weinheim, Germany)* **1997**, *9*, 138. (b) Hubbard, S. F.; Petschek, R. G.; Singer, K. D.; D'Sidocky, N.; Hudson, C.; Chien, K. D.; Henderson, C. C.; Cahill, P. A. *J. Opt. Soc. Am.* **1998**, *B15*, 289. (c) Nalwa, H. S.; Watanabe, T.; Miyata, S. *Adv. Mater. (Weinheim, Germany)* **1995**, *7*, 754.

(28) Zhang, N.; Jiang, M. H.; Yuang, D. R.; Xu, D.; Tao, X. T.; Shao, Z. S. J. *J. Cryst. Growth* **1990**, *102*, 581.

(29) Tao, X.; Zhang, N.; Yuang, D.; Xu, D.; Yu, W.; Jiang, M. *Proc. SPIE-Int. Soc. Opt. Eng.* **1990**, *1337*, 385.

(30) (a)Whitaker, C. M.; Patterson, E. V.; Kott, K. L.; McMahon, R. I. *J. Am. Chem. Soc.* **1996**, *118*, 9996. (b) Moylan, C. R.; Twieg, R. J.; Lee, V. Y.; Swanson, S. A.; Better, K. M.; Miller, R. D. *J. Am. Chem. Soc.* **1993**, *115*, 12599. (c) Verbiest, T.; Burland, D. M.; Jurich, M. C.; Lee, V. Y.; Miller, R. D.; Volksen, W. *Science* **1995**, *268*, 1604.

(31) Singer, K. D.; Kuzyk, M. G.; Holland, W. R.; Sohn, J. E.; Lalama, S. J.; Comizzoli, R. B.; Katz, H. E.; Schilling, M. L. *Appl. Phys. Lett.* **1988**, *53*, 1800.

(32) Burland, D. M.; Miller, R. D.; Walsh, C. A. *Chem. Rev.* **1994**, *94*, 31.

(33) Suzuki, A.; Matsuka, Y. *J. Appl. Phys.* **1995**, *77*, 965.

(34) Singer, K. D.; King, L. A. *J. Appl. Phys.* **1991**, *70*, 3251.

(35) Michellotti, F.; Toussaere, E.; Levenson, R.; Liang, J.; Zyss, J. *J. Appl. Phys*. **1996**, *80*, 1773.